

Expanded View Figures

Figure EV1. Tissue-specific proteomic analysis in *Drosophila*.

- A Correlation heatmap (Pearson's correlation coefficient) across all tissues (thorax, gut, fat body and brain) and all genotypes (A: w^{Dah} , B: $dfoxo^{A94}$, C: *InsP3-Gal4/UAS-rpr* and D: *InsP3-Gal4/UAS-rpr, dfoxo^{A94}*).
- B Tissue-specific PCA plots showing inter-genotype clustering of individual samples.
- C Tissue-specific MA plots of log₂ fold change and average expression level (LFQ) for all detected (black) and significantly regulated (orange) proteins between *InsP3-Gal4/UAS-rpr* vs. w^{Dah} flies (FDR = 0.1).
- D Tissue-specific volcano plots of $-\log_2 P$ -value (adjusted) and log₂FC for all detected (black) and significantly regulated (orange) proteins between *InsP3-Gal4/UAS-rpr* vs. w^{Dah} flies (FDR = 0.1).

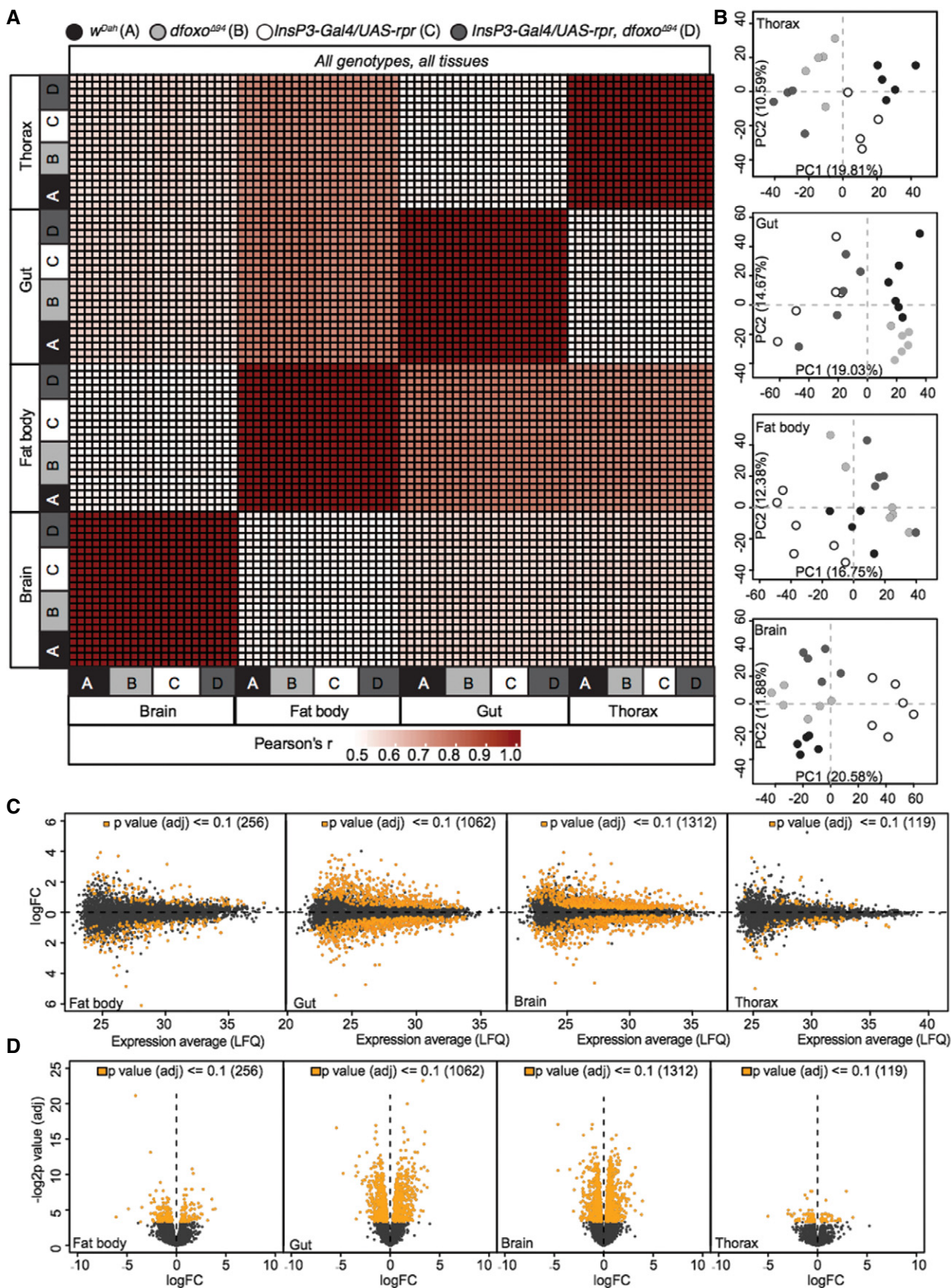


Figure EV1.

Informatic work flow scheme

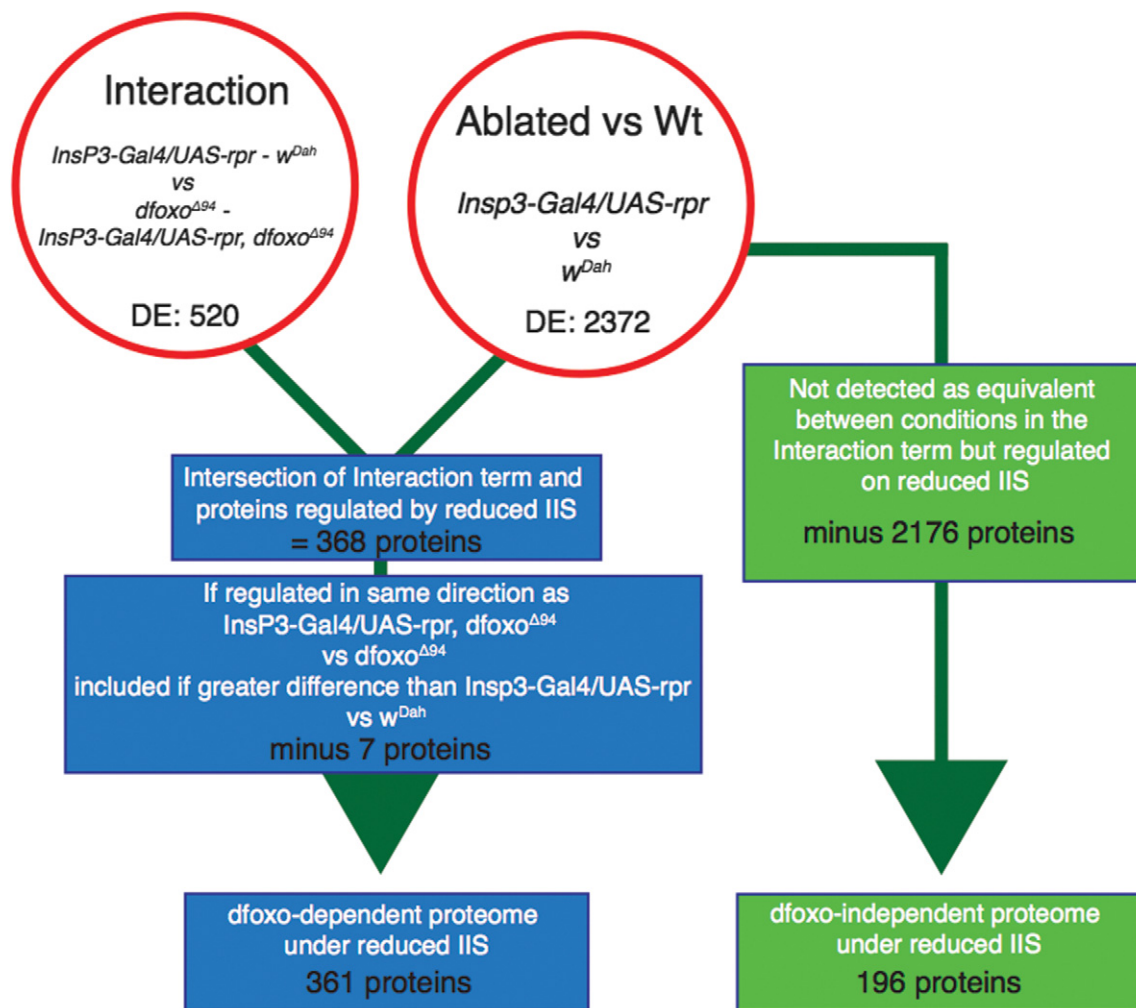


Figure EV2. Bioinformatic scheme for determining *dfoxo*-dependent and -independent protein expression under reduced IIS.

Genotypes defined as w^{Dah} , $dfoxo^{\Delta94}$ mutant, $InsP3-Gal4/UAS-rpr$ and $InsP3-Gal4/UAS-rpr, dfoxo^{\Delta94}$. Reduced IIS-mediated changes in the wild-type background ($InsP3-Gal4/UAS-rpr$ vs. w^{Dah}) and in the $dfoxo^{\Delta94}$ background ($InsP3-Gal4/UAS-rpr, dfoxo^{\Delta94}$ vs. $dfoxo^{\Delta94}$) or their interaction term ($InsP3-Gal4/UAS-rpr - w^{Dah}$ vs. $InsP3-Gal4/UAS-rpr, dfoxo^{\Delta94} - dfoxo^{\Delta94}$). *dfoxo*-dependent proteins were defined as proteins regulated between $InsP3-Gal4/UAS-rpr$ and w^{Dah} and within the interaction term ($InsP3-Gal4/UAS-rpr - w^{Dah}$ vs. $InsP3-Gal4/UAS-rpr, dfoxo^{\Delta94} - dfoxo^{\Delta94}$), but also if the expression response was the same in $InsP3-Gal4/UAS-rpr$ vs. w^{Dah} and $InsP3-Gal4/UAS-rpr, dfoxo^{\Delta94}$ vs. $dfoxo^{\Delta94}$ providing the response was greater in $InsP3-Gal4/UAS-rpr$ vs. w^{Dah} . Proteins were identified as *dfoxo*-independent if they were regulated between $InsP3-Gal4/UAS-rpr$ and w^{Dah} , and were not subject to interaction effects (equivalence given a tissue-specific threshold). Also included were proteins with a stronger same directional response in $InsP3-Gal4/UAS-rpr, dfoxo^{\Delta94}$ vs. $dfoxo^{\Delta94}$ than in $InsP3-Gal4/UAS-rpr$ vs. w^{Dah} , regardless of interaction. See Materials and Methods section for full descriptions.

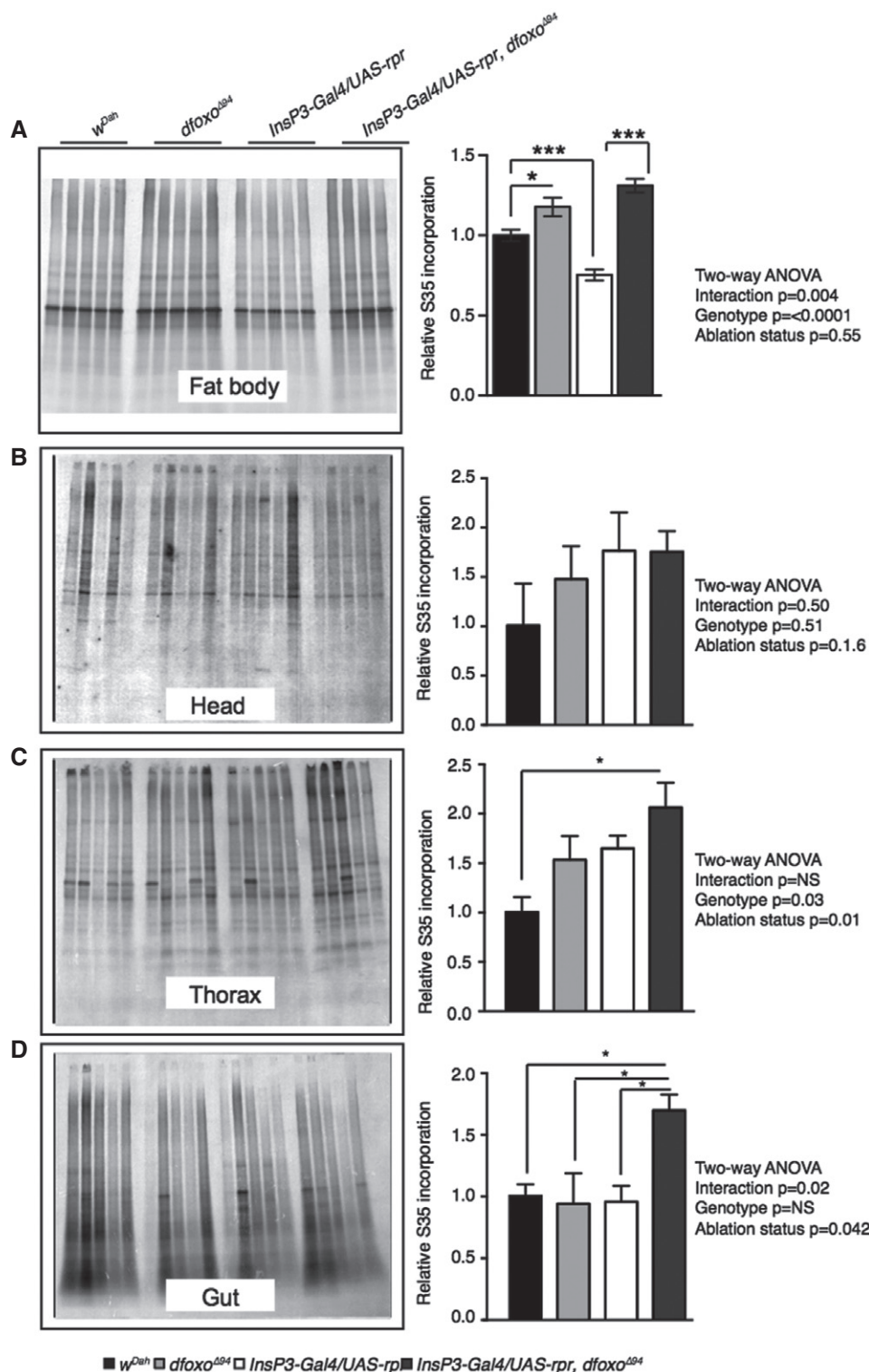


Figure EV3. Translational activity in the fat body under reduced IIS is reduced in a *dfoxo*-dependent manner.

A–D *De novo* protein synthesis as measured by incorporation of ^{35}S into proteins from *ex vivo* (A) fat body, (B) head, (C) thorax and (D) gut tissue. Equal levels of protein were loaded per lane. Representative gel exposures show fat body ^{35}S incorporation from *w^{Dah}*, *dfoxo^{Δ94}*, *InsP3-Gal4/UAS-rpr* and *InsP3-Gal4/UAS-rpr, dfoxo^{Δ94}* flies. Quantification of gel exposures normalized to total protein and corresponding two-way ANOVA, as well as Bonferroni corrected *post hoc* tests are shown alongside each gel exposure. Error bars show SEM, $n = 11$ for *w^{Dah}* and *InsP3-Gal4/UAS-rpr* fat body samples, for all other genotypes and tissues $n = 5$, * $P < 0.05$, *** $P < 0.001$.

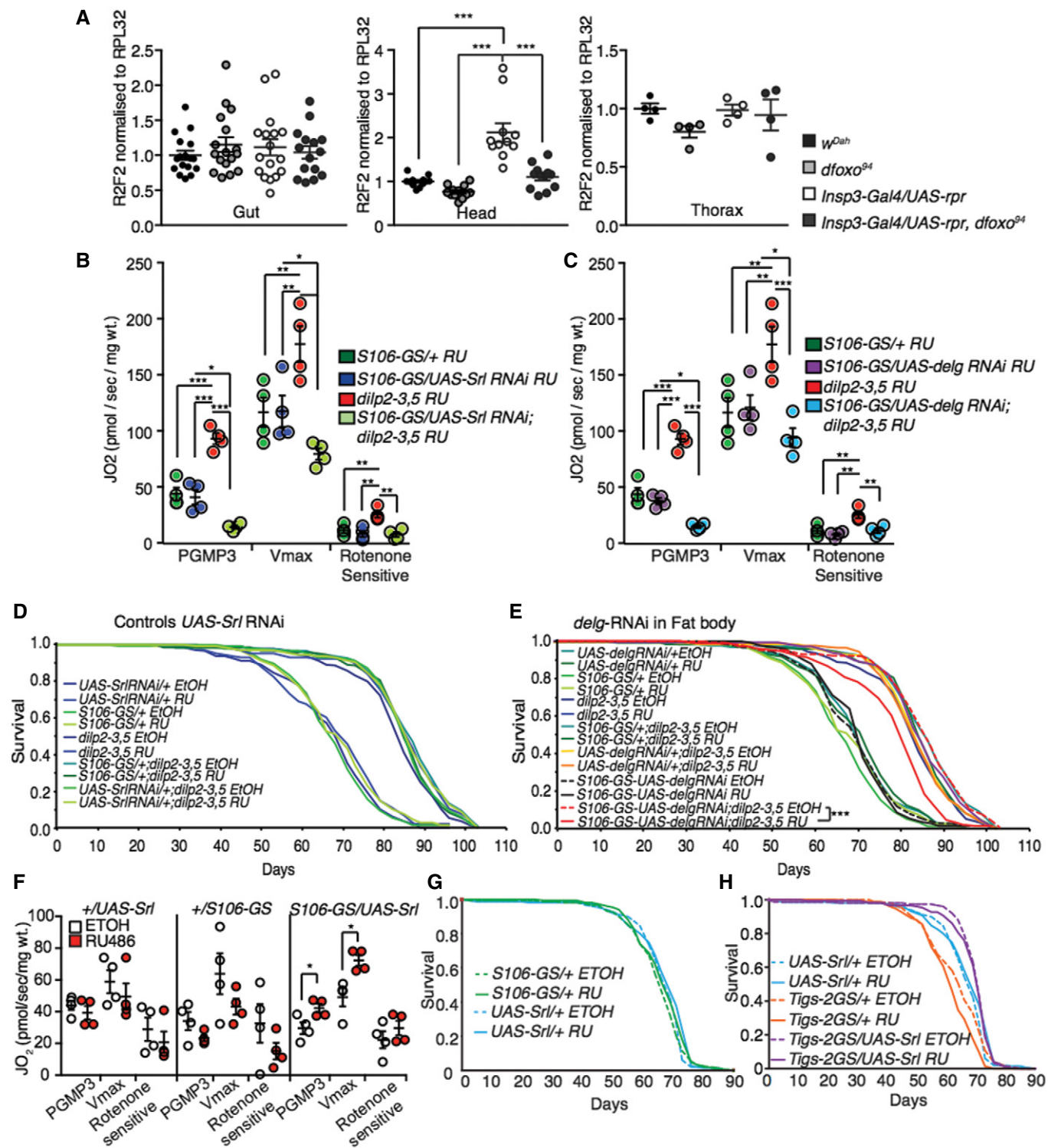


Figure EV4.

Figure EV4. Reduced IIS does not regulate mtDNA levels in the gut or head.

- A Relative mtDNA levels compared to nuclear DNA in the gut ($n = 17$), head ($n = 12$) and thorax ($n = 4$). Fat body mtDNA levels shown in Fig 5E, significance determined by two-way ANOVA.
- B, C Fat body oxygen consumption normalized to dry wt. of flies with fat body-specific reduction of either (B) *Spargel* levels (*S106GS/UAS-Srl RNAi* + RU) ($n = 4$) or (C) *delg* (*S106GS/UAS-delg RNAi* + RU) in the presence and absence of *dilp2-3,5* and genetic controls ($n = 4$), significance determined by two-way ANOVA. Oxygen consumption was assessed by using substrates entering the level of complex I (PGMP3), complex I+II once uncoupled by CCP (Vmax) and rotenone-sensitive complex I+II + rotenone ($n = 4$), significance determined by two-way ANOVA.
- D Lifespan analysis of genetic control flies with fat body-specific reduction in *Spargel* levels (*S106-GS/UAS-Srl RNAi* + RU) (Fig 4F) ($n > 150$).
- E Lifespan analysis of *dilp2-3,5* mutant and control flies with reduced expression of *Delg* in the fat body (*S106-GS/UAS-Delg RNAi*) induced by RU or none induced ($n = 150$). Statistical significance was determined by Log Rank test.
- F Fat body oxygen consumption normalized to dry wt. of flies with induced (RU) or non-induced (EtOH) fat body-specific over-expression of *Spargel* (*S106GS/UAS-Srl*) and genetic controls (+*UAS-Srl* and +*S106GS*) ($n = 4$), significance determined by one-way ANOVA.
- G Lifespan analysis of genetic control flies from over-expression of *Spargel*, specifically in the adult fat body (Fig 4G) ($n = 150$).
- H Lifespan analysis of flies with induced (RU) or non-induced (EtOH) over-expression of *Spargel* in the adult gut (*Tigs-2GS/UAS-Srl*), along with genetic controls ($n = 150$).

Data information: Error bars indicate mean SEM (* $P < 0.05$; ** $P < 0.01$; *** $P < 0.001$).

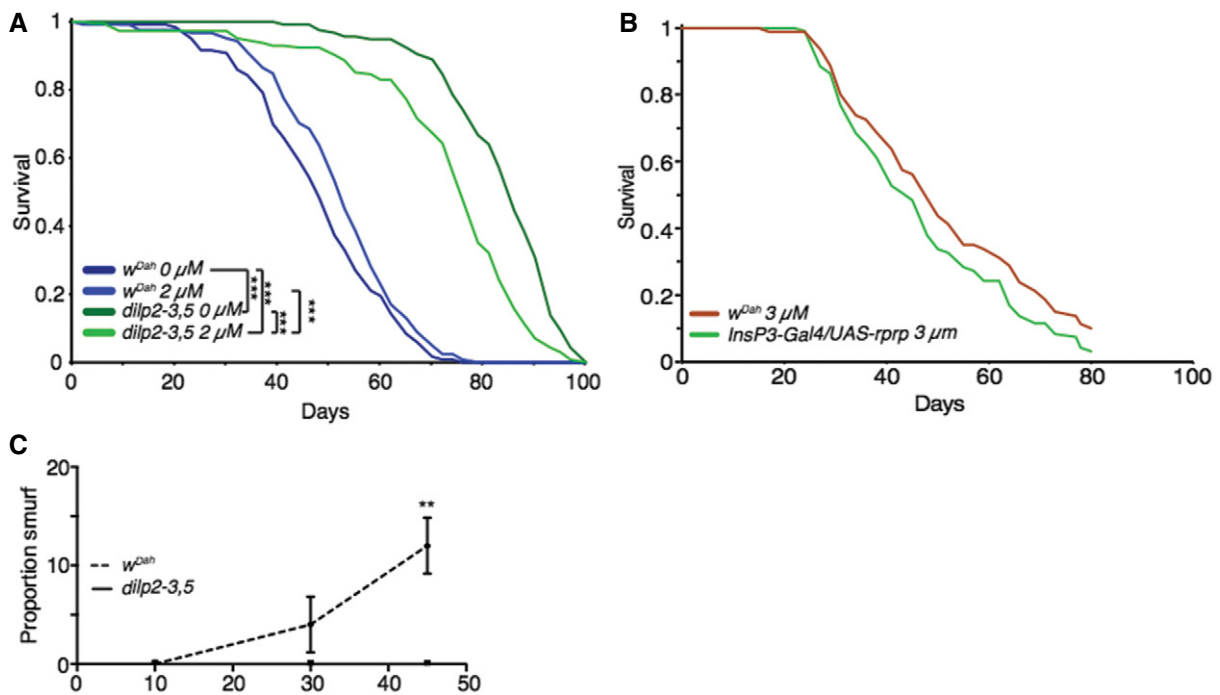


Figure EV5. Proteasome activity is necessary for IIS-mediated longevity, in an independent model of reduced IIS.

- A Lifespan analysis of control flies (w^{Dah}) and *dilp2-3,5* mutant flies treated with 2 μM proteasome inhibitor (bortezomib) or vehicle (EtOH) ($n > 125$). Statistical significance was determined by Log Rank test.
- B Lifespan analysis of wild-type flies (w^{Dah}) and mNSC-ablated flies treated with 3 μM proteasome inhibitor (bortezomib) ($n > 80$).
- C Assessment of age-related gut integrity through “Smurf” assay at different ages (10, 30, 45 days) in wild-type flies (w^{Dah}) and *dilp2-3,5* mutant flies ($n = 100$), significance determined by t-test at each age.

Data information: Bars indicate mean SEM (** $P < 0.01$; *** $P < 0.001$). For associated lifespan, see Fig 6.

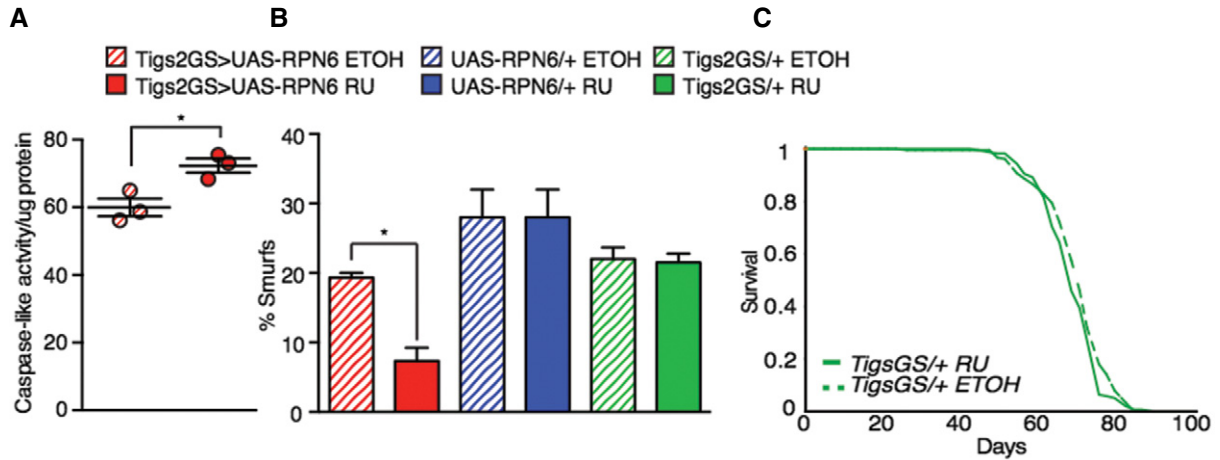


Figure EV6. Control lifespan analysis for adult gut-specific expression of proteasomal subunit RPN6, proteasomal activity and gut integrity.

A Gut proteasome activity (caspase-like) of *Tigs2-Geneswitch/UAS-RPN6* flies compared to *+UAS-RPN6* control flies ($n = 3$), significance determined by *t*-test.

B Assessment of gut integrity through “Smurf” assay (65 days) between induced (RU treated) and uninduced (ETOH treated) *Tigs2-Geneswitch/UAS-RPN6* ($n = 200$) flies and induced (RU treated) and uninduced (ETOH treated) driver controls *Tigs2-Geneswitch/+* ($n = 200$) and *UAS (+UAS-RPN6, n = 75)* control flies.

C Gut-specific driver (*Tigs-Gal4-GS/+*) control lifespan in the presence of RU486 (200 μ m) or vehicle (EtOH) ($n > 180$).

Data information: Bars indicate mean SEM ($*P < 0.05$).

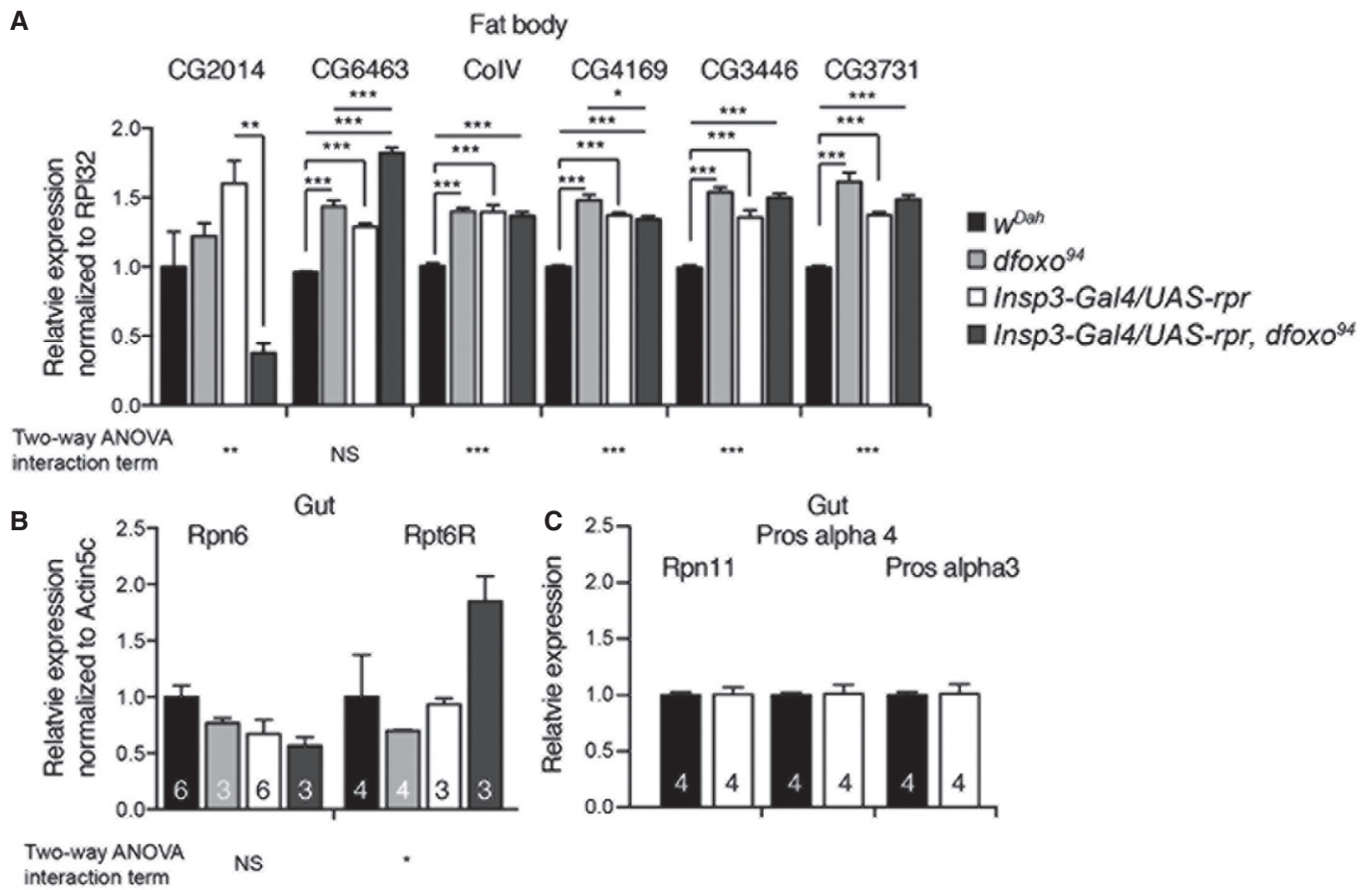


Figure EV7. qRT-PCR analysis of tissue-specific candidate gene expression in response to reduced IIS.

A–C qRT-PCR analysis shows gene expression levels of *CG2014*, *CG6463*, *CoIV*, *CG4169*, *CG3731* in the fat body (A), or of *Rpn6*, *Rpt6R*, *Rpn11* and *Pros-alpha3* in the gut (B, C) of control (*w^{Dah}*), *dfoxo* mutant (*dfoxo⁹⁴*), mNSC-ablated (*Insp3-Gal4/UAS-rpr*) and mNSC-ablated flies in the absence of *dfoxo* (*Insp3-Gal4/UAS-rpr, dfoxo⁹⁴*). Relative expression levels are normalized to either RPL32 (A) or Actin5c (B, C). Significance established by two-way ANOVA and *post hoc* pairwise tests ($n = 3$, or otherwise shown). Bars indicate mean SEM (* $P < 0.05$; ** $P < 0.01$; *** $P < 0.001$).